

## **APPENDIX 4.7.2.A**

# **OH SUPPRESSION – CURRENT STATUS AND FUTURE PROSPECTS**

Report prepared for the New Initiatives Office, 2001.

## APPENDIX 4.7.2 A

### OH SUPPRESSION—CURRENT STATUS AND FUTURE PROSPECTS

With the exception of a few strong absorption bands, the sky in the near-infrared is relatively transparent but very bright. From 0.9 through 1.8 microns, the sky brightness is due to line emission from molecules and ions in the upper atmosphere, mostly OH. Beyond about 2.2 microns, it is dominated by thermal emission. The mean sky brightness in magnitudes/arcsec is roughly 15.6 in the *J*-band and 13.8 in the *H*-band. In addition to being bright, the emission is strongly variable, making sky subtraction difficult beyond the inevitable shot noise associated with the sky emission.

The OH lines are very narrow (unresolved at a resolving power of 17,000), and although the strong ones are numerous (53 in *J*, 69 in *H*), they are not beyond the reach of case-by-case suppression. However, once suppressed, there is still an underlying continuum of somewhat uncertain amplitude and origin. Table 1 summarizes the data and sources. We have not found a recent measurement for the continuum at *J*. The value quoted is the lowest value found.

**Table 1** Sky background emission.

Band	? [μ]	?? [μ]	Ave. Line flux density [ ? s <sup>-1</sup> m <sup>-2</sup> arcsec <sup>-2</sup> μ <sup>-1</sup> ]	Ave. Cont. flux density [ ? s <sup>-1</sup> m <sup>-2</sup> arcsec <sup>-2</sup> μ <sup>-1</sup> ]	% line flux	Data source
I	0.85		?	130		Noxon (1978)
J	1.25	0.22	1.6e04	310	52%	Sobolov (1978)
H	1.665	0.28	2.6e04	590	44%	Maihara (1993)

Suppressing or avoiding the effects of the OH emission has received attention from many authors (see References 1-4 at the end of this appendix). In this review, we summarize the important results and look at some of the implications for instrument design.

Schemes to suppress the OH emission in astronomical observations can be divided into two classes: filter suppressors and dispersive suppressors.

#### FILTER SUPPRESSORS

Herbst<sup>5</sup> has considered the possibility of designing in-line filters for suppressing the flux due to OH line emission. His conclusions are disappointing. Leaving aside the daunting technical task, he finds that the form and efficiency of practically realizable filters do not improve the performance.

Keller<sup>6</sup> has proposed to use the phenomenon of spectral hole burning in an optical medium as a filter for OH suppression. This interesting concept is far from practical realization, and for that reason, we have not analyzed it further here. However, it would be interesting to understand the extent to which it overcomes the questions of efficiency raised by Herbst.

#### DISPERSIVE SUPPRESSORS

In a dispersive suppressor, the light is dispersed in space to physically separate the OH-contaminated light from the uncontaminated light. At this point, the light can be: (1) detected directly, and the two classes of pixels are treated separately in software (the contaminated pixels are discarded, and the uncontaminated ones are co-added to achieve greater *s/n* ratio); or (2) masked and then recombined in optically—in hardware—to produce a lower resolution spectrum.

The latter technique has the advantage of avoiding the per-pixel noise sources of dark current and read noise. (The importance of this effect will be discussed further in this appendix.) With the hardware suppressor, there is also a tradeoff between greater complexity in optics (mask, recombining optics) and the reduced requirement for detector real estate.

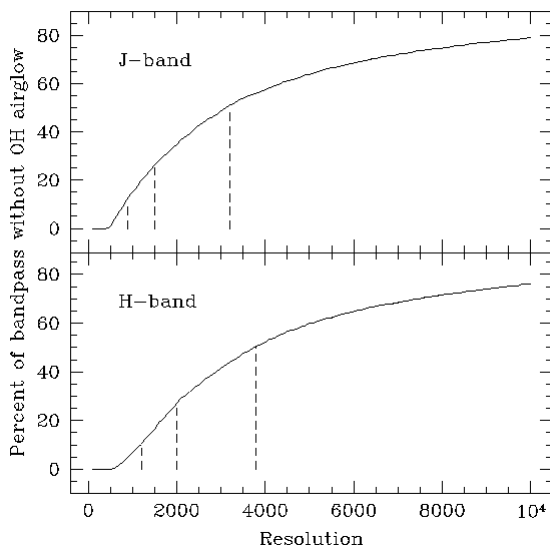
It is also conceivable to sample, disperse, mask, and then completely recombine the light of an image, suppressing all spectral information to give priority to  $s/n$  enhancement of the purely spatial information.

## PERFORMANCE

In principle, given the low intrinsic width of the OH lines, the fraction of the band contaminated by them is very small. If we take the intrinsic width to be  $< R = 100,000$ , the fraction of the band contaminated amounts to  $< 2\%$ . However, there are several effects that lead to diminishing returns as one attempts to decrease the number of contaminated resolution elements by increasing the spectral resolution:

- Continuum background—Some of this is intrinsic to the sky, but one should also include a factor for imperfect rejection of the suppressed lines due to scattering in the instrument (perhaps 1-2% of the integrated emission line intensity) that will be added to the sky continuum.
- Read noise.
- Dark current.
- Cost of spectrograph.

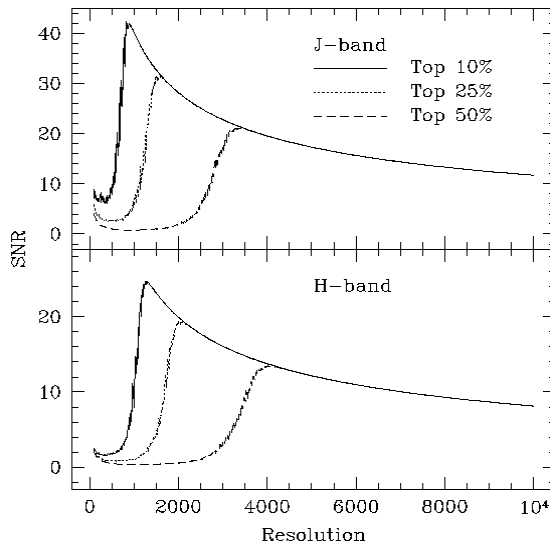
The recent and continuing increase in the size and affordability of arrays and improvements in both read noise and dark current have tended to diminish the importance of the last three items on the list. As long as they are of negligible importance, there is no advantage to recombining the dispersed light before detection. This is the optimal situation: the flexibility to choose the spectral resolution one wants, even after detection, without compromise in noise performance. This situation almost prevails in visible spectroscopy, but in the near-IR, there is still a significant tradeoff between spectral resolution and ultimate noise performance.



Martini et al.<sup>7</sup> have presented a numerical simulation of the software technique of avoiding or suppressing OH contamination. They consider the performance of a conventional spectrograph as a function of spectral resolution. They define an uncontaminated pixel as one whose  $s/n$  is degraded no more than 10% by the effect of line emission. Figure 1 shows the growth in the percentage of pixels that are uncontaminated as a function of the spectral resolution.

**Figure 1** OH contamination versus spectral resolution.

The dashed lines show the resolutions at which 10, 25, and 50% of the pixels are uncontaminated. The  $s/n$  ratio of these groups of pixels is evaluated for particular assumptions about the source and noise contributions.



In Figure 2, Martini et al. show the  $s/n$  of subsets of the pixels achieved as a function of resolution as a larger fraction of the pixels becomes uncontaminated. They then analyze the resolution that maximizes the signal-to-noise for a hypothetical measurement in which the final rebinned resolution is  $R = 500$ .

**Figure 2** Signal-to-noise ratios.

The lesson of Martini's work is that, depending on the science requirements (what fraction of the band contains spectral information, as opposed to mere flux), it may be advantageous to over-disperse and then co-add pixels that are uncontaminated by OH flux. The optimal amount of over-dispersion depends on the spectral resolution desired; there is no single optimum.

## COMPARISON WITH HARDWARE DISPERSIVE SUPPRESSORS

A hardware dispersive suppressor is a spectrograph where high dispersion and masking of OH features takes place before detection of light at a lower final dispersion. To make the comparison concrete, we compare the performance of the Subaru hardware compression instrument with a hypothetical software-based suppressor. The comparison will be detail-specific; the general result is valid, but the point of crossover in performance will depend on implementation.

The hardware suppressor's potential is realized in the extreme low-flux limit, where shot noise in the source or background flux is comparable to the read noise or dark-current noise in exposure. With the latter noise sources is the noise incurred per pixel, so spreading the light over any more than the minimum required number of pixels loses efficiency.

The dispersion required is set by the science. The study of isolated emission lines may require high resolution to avoid contamination of the lines of interest, but nothing is gained by de-dispersing the light to a lower resolution. The hardware suppressor is useful where a significant number of spectral resolution elements contain useful flux, but where the resolution required is not high. To illustrate that kind of application, we compare the use of hardware and software suppression in the case of two final resolutions  $R = 500$  and  $5$ , respectively. The parameters in Table 2 are fixed in the comparison.

**Table 2** Parameters used in simulations.

The results are summarized in Figures 3-6 for each of the two resolutions,  $R = 5$  and  $500$  in the  $J$ - and  $H$ -bands, respectively. Within each graph, the results of the different measurement strategies for obtaining the data are compared:

Parameter	Value
Telescope diameter	30 m (no obscuration)
Read noise	10 e-
Dark current	0.1 e-/sec
Integration time	3600 sec
Subaru mask throughput	0.4
Slit area	0.001 arcsec <sup>2</sup>
J flux at 0 mag	$3.07 \cdot 10^{-12} \text{ W nm}^{-1} \text{ m}^{-2}$
H flux at 0 mag	$1.2 \cdot 10^{-12} \text{ W nm}^{-1} \text{ m}^{-2}$

- Unsuppressed
- Subaru-type suppressor
- Perfect filter (doesn't exist!)
- Binning from  $R = 1000$  to final  $R$
- Binning from  $R = 2000$  to final  $R$
- Binning from  $R = 4000$  to final  $R$

The results are plotted as a function of the source brightness in the aperture in magnitudes. The resulting  $s/n$  obtained at the final resolution is normalized by the ideal result that would be obtained with a perfect filter that eliminated the OH lines from the atmosphere. The numerical value of the  $s/n$  for that fiducial case is plotted against a scale on the right-hand axis.

The important result is that, because of the larger throughput loss, the software avoidance technique is uncompetitive only in the very faint, low signal-to-noise limit.

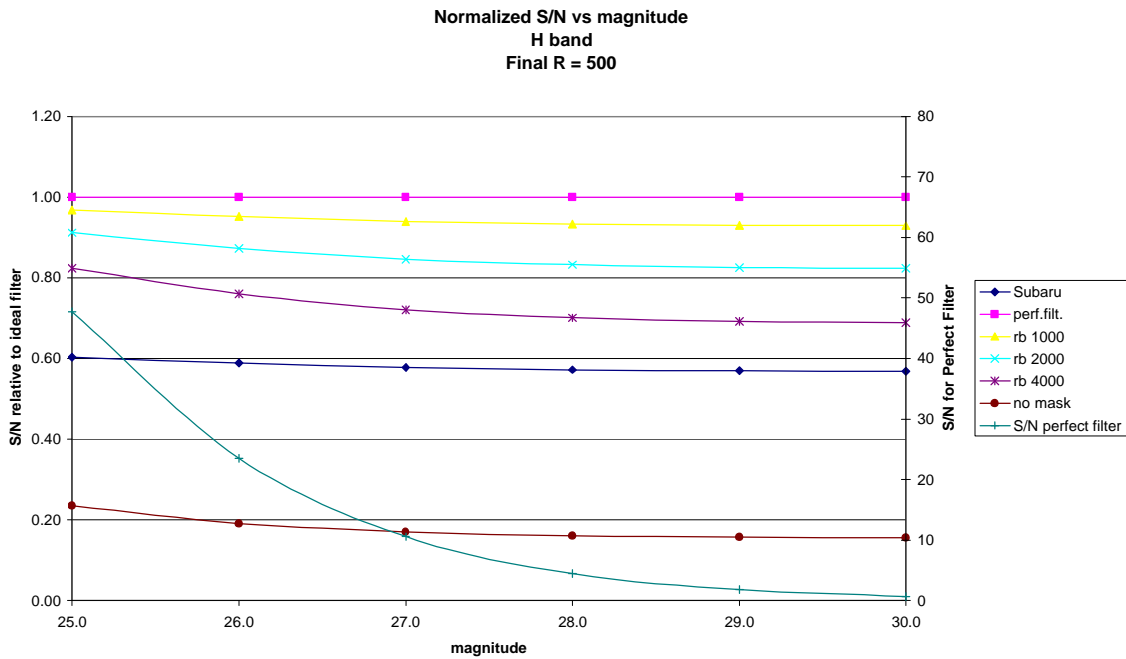


**Figure 3** *H*-band: Final spectral resolution 500. Comparison of different OH rejection strategies.

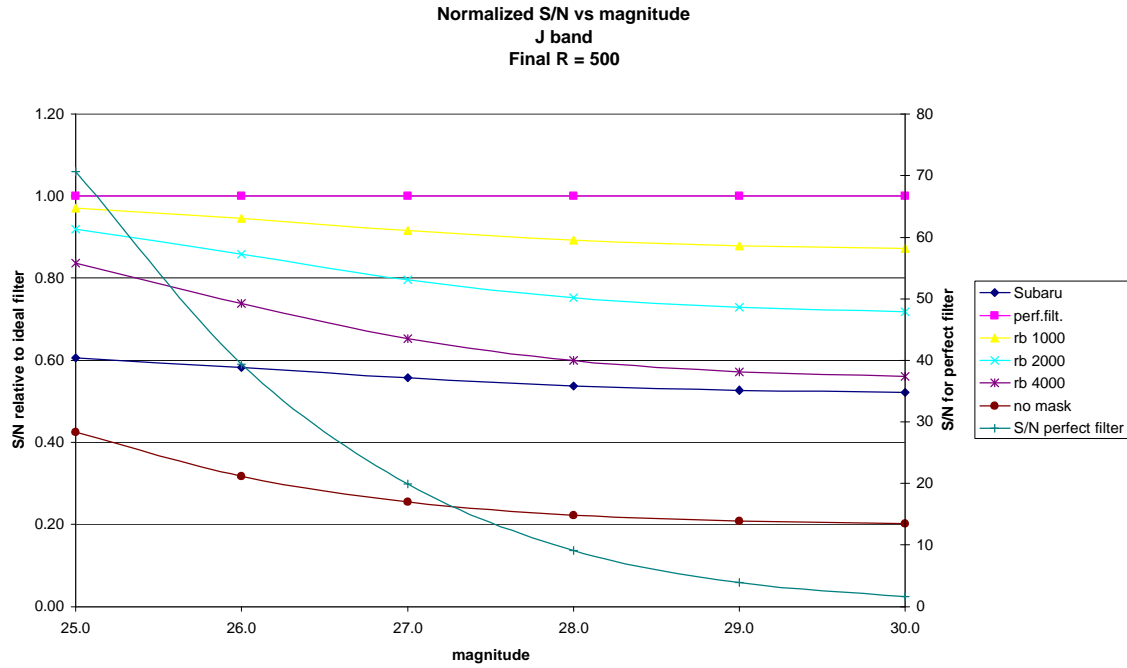


**Figure 4** *J*-band: Final spectral resolution 500. Comparison of different OH rejection strategies.

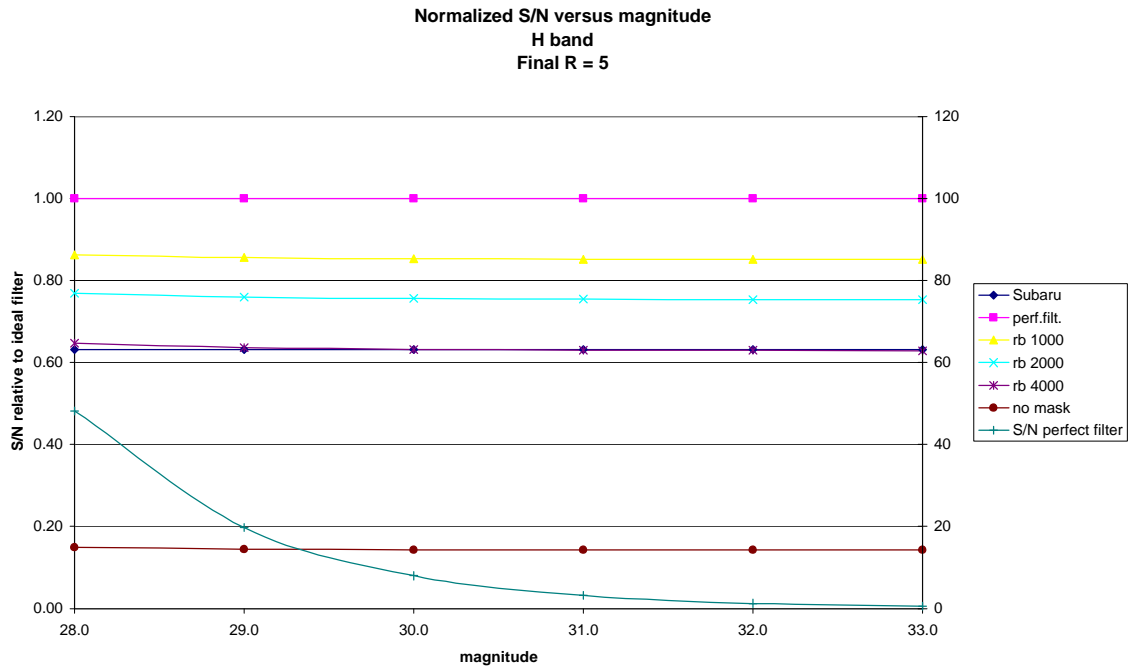


**Figure 5** *H*-band: Final spectral resolution 5. Comparison of different OH rejection strategies.

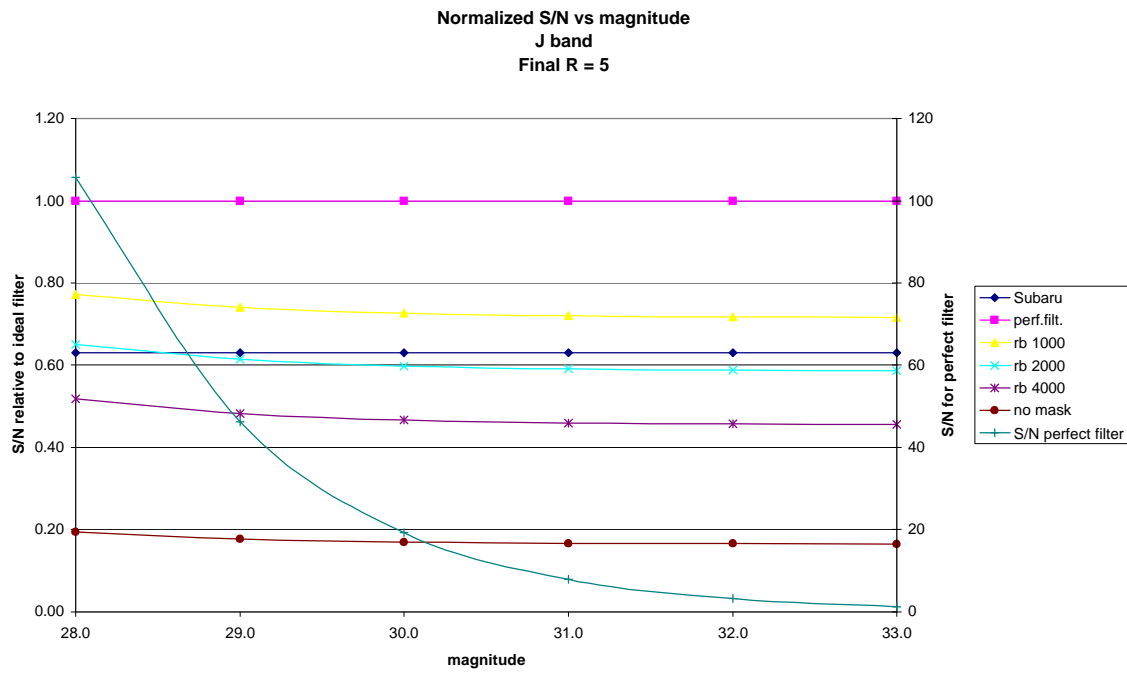


**Figure 6** J-band: Final spectral resolution 5. Comparison of different OH rejection strategies.

## **IMAGING WITH DISPERSIVE SUPPRESSORS**

Although the gains of the software dispersive suppressors are very considerable, the cost of implementation is high. A simple comparison shows that, for imaging, in many practical cases the dispersive suppressor is not an attractive alternative to a simple, broad-band staring array camera in survey mode, operating without suppression.

Consider a relatively wide-field near-IR imager with a 4k x 4k detector array. Given the current costs of purchasing and implementing such detectors, the cost of the detector systems represents a large fraction of the cost of the instrument that might support such a detector. This 16-Mpixel detector is capable of observing roughly  $4 \cdot 10^6$  spatial resolution elements simultaneously.

For an OH-suppressed imager with suppression in software and the same number of detector pixels, the price is clearly greater. How much greater isn't too important for this argument, but the cost of the optics and the much larger instrument required to accommodate dispersion in hardware is probably at least several times more than that of the simple re-imaging dewar and filter assembly in the first instrument. Price aside, how does the performance compare?

To make the comparison, we have to know more about what science is involved. How much of the band in question has to be sampled to make a good estimate of the broad-band flux in the object? This requires analysis case by case. For the purposes of an estimate, we make the optimistic assumption that the band will be adequately sampled with a detected resolution of  $R = 1000$ , which gives about 7% of the band free of OH.

Thus, for each four pixels of spatial resolution,  $2 \times 2000$  pixels are required to produce the required  $R = 1000$  dispersion, Nyquist sampled, for efficient OH avoidance. The 16 Mpixels could be used to observe 4000 spatial resolution elements in this way. From the  $R = 5$  simulation above, we see that  $s/n$  is improved over broad-band imaging by a factor of about 5.4, depending weakly on the object magnitude.

To reach the same  $s/n$  as the broad-band imager, the integration time is reduced by  $(5.4)^2$ , so in the same total integration time, the OH-suppressed imager can observe  $1.2 \cdot 10^5$  spatial resolution elements. The imager wins by a factor of 33. Recall that this doesn't include the extra cost of building the suppressor.

The Subaru hardware suppressor design is not immediately adaptable to a 2-D field, although in principle, an optical system (e.g., an image slicer) could be found to disperse, mask, and then recombine the OH-suppressed light. The optical challenge is daunting for a large field. To my knowledge, no wide-field, dispersive, hardware-suppressed imager has been proposed. I suspect that the unsuppressed imager will continue to be more cost-effective for imaging in survey mode.

## **IFU SPECTROMETERS—A USEFUL MIDDLE GROUND**

Pointed observations are another matter, and are well-adapted to the concept of N-deployable integral field units (IFUs) with OH suppression in software. Here we sacrifice field coverage in the interest of efficient observation of N pre-selected sub-fields. Sources, which could be identified at the 3-sigma level with the imager, could then be followed up with the IFU spectrometer, and (reconstituted) broad-band photometry could be performed on the same objects, with OH-suppression to a  $s/n$  of about 15 in the same time.

## **THE CASE OF MEIFU**

An interesting case to consider is that of the proposed instrument MEIFU (million element integral field unit) that will consist of a million spatial pixels, each dispersed. In this case, the entire field of

view is covered with pixels, so there is not an issue of trading off spectral resolution elements for more spatial ones. The concept is presented briefly in Section 4.7.5. The target science for MEIFU is not particularly well-addressed by either a deployable IFU or a broad-band imager: finding Lyman alpha emission line objects at large redshift. Thus, the object of the science is to discover emission line objects of which neither the position nor the wavelength is known a priori. For such a program there is a strong disadvantage in observing broad-band on the one hand and low efficiency with a deployable IFU on the other. Because the science potential is large, we propose study of the potential of a MEIFU-like instrument for the GSMT.

## FOLLOW-ON STUDIES

The present study can be extended in several ways. Specifically, we propose to extend the performance evaluation to the *R*-band, where the difficulty of using AO to increase the image contrast against background is much greater. We also plan to include good spectral modeling tools in the Integration Time Calculator (under development) to simulate the efficiency of observing specific science target spectra against realistic sky spectra, to test OH rejection algorithms. Finally, we propose further evaluation of the spectral hole burning technique for constructing filter suppressors of OH lines.

## REFERENCES

---

<sup>1</sup> Iwamuro, F., Motohara, K., Maihara, T., Hata, R., Harashima, T., OHS: OH-Airglow Suppressor for the Subaru Telescope, *PASJ*, **53**, 355-360, 2001.

<sup>2</sup> Maihara, T., Iwamuro, F., Yamashita, T., Hall, D.N.B., Cowie, L.L., Tokunaga, G.A.T., Pickles, A., *PASP*, **105**, 940, 1993.

<sup>3</sup> Noxon, J.F., *Planet. Space Sci.*, **26**, 191, 1978.

<sup>4</sup> Sobolev, V.G., *Planet. Space Sci.*, **26**, 703, 1978.

<sup>5</sup> Herbst, T.M., Numerical Evaluation of OH-Suppression Instruments, *PASP*, 106, 1298-1309, Dec. 1994.

<sup>6</sup> Keller, C.U., "5000 by 5000 Spatial by 15000 Spectral Resolutions Elements: First Astronomical Observations with a Novel 3-D Detector", in *Imaging the Universe in Three Dimensions*, ASP Conf. Ser., **195**, 495, 2000.

<sup>7</sup> Martini, P., DePoy, D., *Proc. SPIE* **4008**, 695-702, 2000.